INTERNATIONAL JOURNAL FOR NUMERICAL METHODS IN FLUIDS
Int. J. Numer. Meth. Fluids 2004; **46**:877–902
Published online 27 September 2004 in Wiley InterScience (www.interscience.wiley.com). DOI: 10.1002/fld.743

Calculation of impulsively started incompressible viscous flows

A. Marra*,†, A. Mola, L. Quartapelle and L. Riviello

Dipartimento di Ingegneria Aerospaziale, Politecnico di Milano, Via La Masa, 34, 20156, Milano, Italy

SUMMARY

The paper's focus is the calculation of unsteady incompressible 2D flows past airfoils. In the framework of the primitive variable Navier–Stokes equations, the initial and boundary conditions must be assigned so as to be compatible, to assure the correct prediction of the flow evolution. This requirement, typical of all incompressible flows, viscous or inviscid, is often violated when modelling the flow past immersed bodies impulsively started from rest. Its fulfillment can however be restored by means of a procedure enforcing compatibility, consisting in a *pre-processing* of the initial velocity field, here described in detail. Numerical solutions for an impulsively started multiple airfoil have been obtained using a finite element incremental projection method. The spatial discretization chosen for the velocity and pressure are of different order to satisfy the inf–sup condition and obtain a smooth pressure field. Results are provided to illustrate the effect of employing or not the compatibility procedure, and are found in good agreement with those obtained with a non-primitive variable solver. In addition, we introduce a *post-processing* procedure to evaluate an alternative pressure field which is found to be more accurate than the one resulting from the projection method. This is achieved by considering an appropriate 'unsplit' version of the momentum equation, where the velocity solution of the projection method is substituted. Copyright © 2004 John Wiley & Sons, Ltd.

KEY WORDS: Navier–Stokes equations; unsteady incompressible flows; impulsive start; compatibility conditions; pressure field

1. INTRODUCTION

The impulsive start of bodies immersed in an incompressible viscous fluid has always been a problem of great fluid dynamic interest, mostly because of the simplicity of its statement, see, for instance, Lighthill [1, Section 6.1, p. 80] and the discussion by Stuart on the implications for the unsteady boundary layer theory [2, Chapter VII, p. 349]. Owing to their idealized nature, these flows represent in fact a special case of evolutive problems where the boundary values are constant for all $t > 0$, cf. Telionis [3, p. 79].

*Correspondence to: A. Marra, Dipartimento di Ingegneria Aerospaziale, Politecnico di Milano, Via La Masa, 34, 20156, Milano, Italy.
†E-mail: Andrea_Marra@hotmail.com

Received 3 June 2003
Revised 16 April 2004

From the viewpoint of the numerical solution, difficulties in the interpretation of the results to these problems have often been encountered, since the computed flows present a complexity disproportioned with the simplicity of their mathematical statement. This has usually been related to the idealized character of impulsive motion, a circumstance that has focused the attention on the physical model of this class of problems, in order to introduce hypotheses able to allow the solution, as described, for instance, by Karamcheti [4, Section 9.9, p. 246] and Ashley and Landahl [5, Chapter 2].

A first intent of this paper is to show that in impulsively started flows a large portion of these difficulties is related to the mathematical consequences of the incompressibility hypothesis on the well-posedness of the dynamic problem. In fact, the analysis of the initial boundary value problem associated with several impulsively started incompressible flows shows that the compatibility condition between the initial and boundary data for the (normal components of) velocity is violated. This does not occur in some very simple problems with purely tangential impulsive motion of the solid boundary, whose prototype is the first Stokes problem. Actually, for general incompressible flows the fulfillment of the compatibility condition, as well as the conditions of solenoidality on the initial velocity field and of zero total flux of the velocity boundary value, is fundamental for the well-posedness of an unsteady problem. In this respect, simple problems with purely tangential motion of the walls cannot be considered representative of the entire class of impulsively started flows.

The theoretical background for the analysis of the problem is provided by Ladyzhenskaya [6] and Temam [7] and includes the aforementioned compatibility condition, which ensures existence and uniqueness of the solution for viscous incompressible flows in spaces of functions of suitable regularity. As a matter of fact, the presence of the compatibility condition for flows in domains of arbitrary shape is due only to the incompressibility hypothesis, and therefore its mathematical consequences are relevant also for non-viscous flows, as it will be seen in the following.

The present paper will show that the well-posedness of the problem for impulsively started flows, governed by the Navier–Stokes equations in the primitive variables pressure and velocity, can be restored by creating a modified initial velocity field, compatible with the boundary value specifications. This procedure leads to a different initial boundary value problem, here solved by means of the second order projection method of Guermond and Quartapelle [8, 9], whose main features are also recalled.

Solutions to problems with compatible or incompatible initial and boundary data will be calculated and compared to clarify that the compatibility conditions not only have a central position in the correct mathematical formulation of unsteady incompressible problems, but also that their respect leads to solutions reproducing the expected behaviour of the flow at the very first instants of the simulation: this aspect cannot be underestimated since solutions developing from incompatible data present non-physical pathologies at the beginning of the simulation that are a consequence of the ill-posedness of the problem.

After the inclusion of the procedure enforcing compatibility, the projection method has been extensively used to solve two-dimensional unsteady incompressible flows around a complex multi-profile airfoil at a relatively low Reynolds number and at high incidence. Some results for the vorticity and pressure distributions are presented. Convergence tests have also been performed on a problem with exact solution to verify that the overall method including the start-up correction procedure achieves the theoretical rates of convergence of the finite element projection method.

Another aspect investigated in the paper is the accurate prediction of the pressure field. As well-known, the inf–sup condition requires different orders of approximation for the variables velocity and pressure, for which parabolic and linear interpolations are here chosen. This means that the computed velocity field contains available information that can be exploited to determine another pressure distribution different from that given by the projection method. In fact, it is possible to resort to the original, i.e. unsplit, momentum balance to obtain an equation with the pressure gradient as the only unknown. Since Lagrangian elements are employed, the viscous term will be expressed as the double curl of velocity with this field computed using a quadratic interpolation. Therefore, the new pressure field can be approximated alternatively by means of either $\mathbb{P}_1$ or $\mathbb{P}_2$ polynomials.

As a whole, the analysis developed in the paper addresses the most typical aspects associated with incompressible CFD (ICFD): the need of correct initial and boundary data, the choice of proper approximations for the primitive variables, both brought about by the presence of the incompressibility constraint, the split character of the fractional-step projection method, the second-order accuracy and unconditional stability of the adopted BDF scheme. The complete solution algorithm to be described, including initial data pre-processing to achieve compatibility and final solution post-processing to obtain an improved pressure field, is based on standard numerical ideas and techniques to the point that we dare hope that this article might be considered as a tutorial introduction to ICFD.

The content of this paper is organized as follows. In Section 2 the complete statement of the incompressible Navier–Stokes problem in primitive variables is presented and specified for the problem of a multiple airfoil impulsively started from rest. Section 3 focuses on the theoretical and practical aspects of the compatibility conditions. In particular, Section 3.1 introduces the set of compatibility conditions to be satisfied by any well-posed problem of incompressible fluid dynamics. In Section 3.2 some reasons why the compatibility condition between the initial velocity and the velocity boundary values have been disregarded sometimes in the literature are also discussed. Section 3.3 illustrates the theoretical and numerical procedures used to have compatible initial and boundary data. Section 4 deals with the numerical side of the problem. In particular Section 4.1 gives a brief description of the second-order projection method used to obtain the solutions shown in the paper and contains an outline of the procedures for computing the vorticity and the streamlines from the velocity field provided by the projection method. In Section 4.2 we introduce the proposed post-processing technique to extract two alternative pressure fields from the computed velocity field. Convergence tests are also performed in Section 4.3 to verify the second order time accuracy of the three level BDF projection method, in suitable norms for velocity and pressure, and to compare the precision of the three possible pressure fields considered in the present paper. In Section 5 the flow field and the three pressure coefficients on the airfoils are compared with the corresponding results provided by a non-primitive variable method [10] and some final results about the importance of respecting the compatibility are presented. The last section is devoted to a few concluding remarks.

2. PROBLEM DEFINITION FOR INCOMPRESSIBLE FLOWS PAST AIRFOILS

Let us consider the time-dependent incompressible Navier–Stokes equations formulated in terms of the primitive variables velocity $\mathbf{u}$ and pressure per unit density p, denoted as

'pressure' throughout, for simplicity. The fluid domain V is assumed to be a two-dimensional region of the plane external to one or more airfoils embedded in an incompressible viscous fluid. The evolution of such a fluid motion is described by the following initial boundary value problem:

Find the velocity $\mathbf{u}$ and the pressure p (up to an arbitrary function of t, which can be added to p) so that

$$\begin{aligned} \frac{\partial \mathbf{u}}{\partial t} + (\mathbf{u}\cdot\nabla)\mathbf{u} &= -\nabla p + \nu\nabla^2\mathbf{u} \\ \nabla\cdot\mathbf{u} &= 0 \\ \mathbf{u}_{|t=0} &= \mathbf{u}_0 \\ \mathbf{u}_{|S} &= \mathbf{b} \end{aligned} \tag{1}$$

where ν is the kinematic viscosity, $\mathbf{u}_0$ is the initial velocity field and $\mathbf{b}$ is the velocity prescribed on the boundary S of V. As far as the regularity of the data is concerned, they are assumed to be smooth enough for the purposes of the subsequent analysis.

We are interested in the problem of the flow past airfoils impulsively started from rest to a constant velocity. Typically, this problem consists in an unbounded volume of fluid, initially at rest, where an immersed body is set in motion at time $t=0$ with a constant velocity, for example, $-\mathbf{U}$ towards the left, as shown in Figure 1. These conditions do not fit within the framework of the Navier–Stokes problem (1) which requires a bounded domain with fixed boundaries for its spatial discretization and numerical solution. The problem with an impulsive start of the body can however be recast in the standard form (1) by the following transformations. First, the unbounded domain is truncated at a large but finite distance from the profile through the introduction of an external closed boundary denoted conventionally by S_{ext}. Then, the dynamics of the fluid is studied in an inertial frame of reference, which translates at the constant speed $-\mathbf{U}$ with respect to the stationary fluid, far from

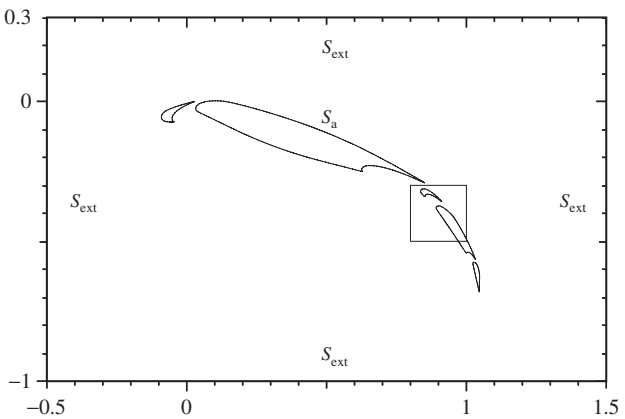

Figure 1. Multiple airfoil in landing configuration and nomenclature of the boundary. The small square is a zoomed area for subsequent representation of numerical solutions.

the airfoil. In this inertial system, the airfoil is immobile for $t>0$, so that its boundary S_a is fixed.

In the new frame of reference the initial flow field will be uniform and equal to $\mathbf{U}$, directed towards the right in the figure. This means that the initial velocity evaluated on the profile S_a will be $\mathbf{U}$, in the new frame. This value is however different from the one prescribed on S_a, denoted by $\mathbf{b}_a$, which must be zero by the no-slip and no-penetration boundary conditions imposed on a fixed rigid wall in viscous flows. A mismatch therefore exists between the information coming respectively from the initial and boundary data, namely $\mathbf{U}=\mathbf{u}_0|_{S_a}\neq\mathbf{b}_a|_{t=0}=0$.

In the following sections we are going to investigate the consequences of this mismatch on the well-posedness of the problem: we will show that there are compatibility conditions and that they must be satisfied to guarantee the well-posedness of the Navier–Stokes problem, once we refer to solutions possessing the lowest admissible regularity, i.e. $\mathbf{u}\in\mathbf{H}^1$, see, Adams [11], for the definition of Sobolev spaces.

3. COMPATIBILITY CONDITIONS AND COMPATIBILIZATION

3.1. Compatibility conditions in unsteady incompressible flows

All the compatibility conditions for the viscous problem depend exclusively on the assumption of the incompressibility of the fluid. Therefore in this section we will discuss their genesis by considering the two physical models assuming a non-viscous or viscous character of the fluid. The first model is associated with the incompressible Euler equations, while the second is given by the incompressible Navier–Stokes equations introduced in Section 2. In both cases the incompressibility of the fluid means here that a uniform and constant density is assumed.

For inviscid incompressible flows, two situations have to be considered, with vorticity vanishing or different from zero. In fact, in a non-viscous fluid, the flow is vortical whenever the initial flow field has a non-zero vorticity, whereas the velocity field remains irrotational whenever the initial vorticity is zero. The latter situation represents an extreme case since the dependence on time is fully contained in the specification of the boundary condition and no initial condition is required for velocity in the mathematical statement of the problem, as shown by Karamcheti [4, p. 249]. Thus, using the well-known property of irrotational fields, the velocity $\mathbf{u}$ in a simply connected domain can be represented at each time $t>0$ as $\mathbf{u}=\nabla\phi$. In this case, the equations governing the irrotational motion of an inviscid and incompressible fluid, together with the boundary condition for the normal velocity, lead to a Neumann boundary value problem for the potential ϕ, in the form of the harmonic problem

$$\nabla^2\phi=0$$
$$\left.\frac{\partial\phi}{\partial n}\right|_S=b_n(\mathbf{r}_s,t) \tag{2}$$

where $b_n(\mathbf{r}_s,t)$ is the normal component of velocity specified on the boundary, to be solved for any $t>0$. As well-known, the Neumann problem for Laplace operator is subjected to a

compatibility condition on its data, which, for a homogeneous equation, reads

$$\oint_S b_n(\mathbf{r}_s, t) = 0 \tag{3}$$

This relation is the only compatibility condition needed for the solution of any irrotational incompressible flow, and its physical interpretation is that the net amount of fluid through the entire boundary must be zero for any $t > 0$.

The second situation of non-viscous incompressible flows corresponds to a rotational or vortical flow. Let us write the equations governing this kind of fluid motion, namely, the incompressible Euler equations:

$$\begin{gathered} \frac{\partial \mathbf{u}}{\partial t} + (\mathbf{u} \cdot \nabla)\mathbf{u} = -\nabla p \\ \nabla \cdot \mathbf{u} = 0 \\ \mathbf{u}(\mathbf{r}, 0) = \mathbf{u}_0(\mathbf{r}) \\ \mathbf{n} \cdot \mathbf{u}(\mathbf{r}, t)|_S = b_n(\mathbf{r}_s, t) \end{gathered} \tag{4}$$

where $\mathbf{u}_0(\mathbf{r})$ is the initial velocity field while $b_n(\mathbf{r}_s, t)$ is the normal component of velocity specified on the whole boundary. Exactly as in the previous case, there is a first compatibility condition requiring a zero net mass flux through the boundary for any $t > 0$, which is expressed by the same global constraint (3). As far as the second condition of compatibility is concerned, it refers only to the initial datum, $\mathbf{u}_0$, and states that the initial velocity field must be solenoidal:

$$\nabla \cdot \mathbf{u}_0 = 0 \tag{5}$$

We can observe that, since the second equation of system (4) represents an instantaneous constraint on $\mathbf{u}(\mathbf{r}, t)$, it seems perfectly legitimate to assume that the same constraint has to be satisfied also at the initial time $t = 0$. Finally, there is a third condition, in which the compatibility between initial and boundary data for the problem is imposed:

$$\mathbf{n} \cdot \mathbf{u}_0|_S = b_n(\mathbf{r}_s, 0) \tag{6}$$

This condition is explained, for instance, by Gresho [12, p. 397], as the application of the incompressibility constraint on the boundary of the initial velocity field: if we consider a thin layer of fluid near a small part of the boundary, the conservation of the local mass flux is assured only if the normal components of the initial and boundary data are equal. From a more physical point of view, the velocity component normal to the boundary must be the same because of the assumption of instantaneous propagation of the normal information and stresses.

The three compatibility conditions above are necessary for demonstrating results of existence and uniqueness of classical solutions to the two-dimensional unsteady Euler equations in a bounded domain and for finite time in suitable spaces of minimal regularity, as shown by Kato [13, p. 189]. Of course, the uniqueness is intended here only up to an arbitrary function of t, which can be added to p. The same compatibility conditions must be respected to guarantee existence and uniqueness also of weak solutions, see the recent textbook by Taylor [14, Theorem 3.2a, p. 489].

Table I.

Time-dependent incompressible flows			
Fluid model	Inviscid and irrotational	Inviscid but rotational	Viscous flows
Governing equations	Laplace equation	Incompressible Euler equations	Incompressible Navier–Stokes
Initial datum		$\mathbf{u}_0(\mathbf{r})$	$\mathbf{u}_0(\mathbf{r})$
Boundary datum	$b_n(\mathbf{r}_s,t)$	$b_n(\mathbf{r}_s,t)$	$\mathbf{b}(\mathbf{r}_s,t)$
Full set of compatibility conditions	$\oint_S b_n(\mathbf{r}_s,t)=0$	$\oint_S b_n(\mathbf{r}_s,t)=0$	$\oint_S \mathbf{n}\cdot\mathbf{b}(\mathbf{r}_s,t)=0$
		$\nabla\cdot\mathbf{u}_0=0$	$\nabla\cdot\mathbf{u}_0=0$
		$\mathbf{n}\cdot\mathbf{u}_0\|_S=b_n(\mathbf{r}_s,0)$	$\mathbf{n}\cdot\mathbf{u}_0\|_S=\mathbf{n}\cdot\mathbf{b}(\mathbf{r}_s,0)$

Finally, we consider the equations governing the viscous model, shown in Section 2, i.e. the incompressible Navier–Stokes equations (1). The initial datum $\mathbf{u}_0$ is prescribed in the whole domain and the entire vector velocity is specified on the boundary for $t\geqslant 0$, differently from the non-viscous case where only its normal component is prescribed. The first compatibility condition is just condition (3), modified in

$$\oint_S \mathbf{n}\cdot\mathbf{b}(\mathbf{r}_s,t)=0 \tag{7}$$

because the prescribed boundary velocity $\mathbf{b}$ is a vector datum in the viscous case. Instead, the presence of viscosity does not affect the mass conservation, so the second condition has the same form (2). Finally, the component of the initial velocity normal to the boundary must be equal to the velocity boundary datum projected on the normal and calculated at $t=0$, namely,

$$\mathbf{n}\cdot\mathbf{u}_0|_S=\mathbf{n}\cdot\mathbf{b}(\mathbf{r}_s,0) \tag{8}$$

The three compatibility conditions above have been shown by Temam [7, p. 253] and Ladyzhenskaya [6, p. 88] to demonstrate the existence of weak solutions of minimal regularity ($\mathbf{u}\in\mathbf{H}^1$) for the incompressible Navier–Stokes problem. The same existence result is quoted also by Taylor, see [14, Theorem 5.9, p. 510] while the additional conditions needed for uniqueness of weak solutions for a finite time are given by Propositions 5.10 and 5.11, p. 511 of Reference [14].

For convenience, the various set of compatibility conditions previously discussed are finally summarized in Table I.

Thus, the same set of compatibility conditions on boundary and initial data holds for the incompressible Euler and Navier–Stokes equations since these conditions are due only to the incompressibility of the fluid, irrespectively of its viscous or inviscid character.

3.2. What is it actually intended by 'an impulsive start'?

Historically, impulsively started flows have been analysed without paying a specific attention to the compatibility between the boundary and initial data. The consequence of their possible

mismatch has often been described as the effect of the instantaneous (because of the incompressibility) propagation of a pressure perturbation, from which the subsequent motion can develop, see, for instance, Telionis [3, p. 81]. This kind of 'physical' interpretation dates back to the earlier analysis due to Lamb of the impulsive generation of motion in an incompressible fluid under quite general geometrical conditions [15, p. 10].

A source of possible difficulty in establishing the correct conditions to be imposed for solving the initial boundary value problems for incompressible viscous flows comes from the central, and unfortunately deceptive, role played by the first Stokes problem. In fact, this problem is often considered the basis for the interpretation of the phenomenon of the whole class of impulsively started flows. This is clearly an incorrect generalization, as it will be shown below.

Let us consider a flat plate of infinite extent that delimits a half space filled by an incompressible viscous fluid initially at rest and assume that the plate can translate only in its own plane. Let us choose a coordinate system with the x axis in the direction of the motion, with the plate located at $y=0$. By the translational invariance in the x direction, $\partial u/\partial x=\partial v/\partial x=\partial p/\partial x=0$, and therefore Equations (1) reduce to the following system for the unknowns $\mathbf{u}=(u,v)$ and p dependent only on y and t:

$$\begin{aligned}\frac{\partial u}{\partial t}+v\frac{\partial u}{\partial y}&=\nu\frac{\partial^2 u}{\partial y^2}\\ \frac{\partial v}{\partial t}&=-\frac{\partial p}{\partial y}+\nu\frac{\partial^2 v}{\partial y^2}\\ \frac{\partial v}{\partial y}&=0\end{aligned}\tag{9}$$

The last equation together with the initial and boundary conditions for the vertical velocity component v, that is, $v(y,0)=0$ and $v(0,t)=0$, gives $v=0$, identically in the entire domain. Thus, in the first Stokes problem the component of velocity normal to the wall, v, vanishes and the compatibility between the initial and boundary values supplementing (9) is trivially fulfilled.

Now, by the second equation of (9), $\partial p/\partial y=0$, so $p=f(t)$, where f is an arbitrary function, and the system reduces to

$$\frac{\partial u}{\partial t}=\nu\frac{\partial^2 u}{\partial y^2}\tag{10}$$

Assuming that the wall is subjected to an impulsive motion with a constant velocity U at time $t=0$, Equation (10) is supplemented by the initial and boundary conditions

$$\begin{aligned}u(y,0)&=0, \quad y>0\\ u(0,t)&=U, \quad t>0\\ u(\infty,t)&=0, \quad t>0\end{aligned}\tag{11}$$

For $t\to 0$ the boundary value for the tangential velocity u does not tend to the initial value, since $U\neq 0$. A discontinuity (although a perfectly admissible one) can exist in the data for the velocity component tangential to the boundary. The problem consisting in Equation (10)

and conditions (11) allows a direct parallelism between the momentum balance Equation (10) and the heat diffusion equation in one dimension, which reads

$$\frac{\partial T}{\partial t} = k \frac{\partial^2 T}{\partial y^2} \tag{12}$$

Unfortunately, this parallelism does not translate in two- and three-dimensional situations, where the heat equation reads

$$\frac{\partial T}{\partial t} = k \nabla^2 T \tag{13}$$

while the equations for incompressible flows, considering for simplicity a linear version of them, become the so-called unsteady Stokes system:

$$\begin{gathered} \frac{\partial \mathbf{u}}{\partial t} = -\boldsymbol{\nabla} p + \nu \nabla^2 \mathbf{u} \\ \boldsymbol{\nabla} \cdot \mathbf{u} = 0 \end{gathered} \tag{14}$$

Since the momentum equation of (14) is parabolic as the temperature equation, one could suppose that the initial values and the boundary values for the velocity are fully independent, as in the first Stokes problem and in the heat equation in one or more dimensions. However, this is not the case because of the incompressibility constraint and of the associated pressure gradient present in the dynamical equation of momentum. In fact, as pointed out in Reference [16], the unsteady incompressible equations (14) for a viscous fluid do define a parabolic problem, but only *after* it has been projected onto the space of solenoidal vector fields tangential to the boundary. This results in taking an initial velocity field and a boundary velocity distribution which satisfy the compatibility conditions. It is worthwhile to note that these conclusions are valid irrespectively of the linear or non-linear character of the equations governing the motion of the incompressible viscous fluid. The same impulsive-flow behaviour characterizing the first Stokes problem is encountered also in more general multi-dimensional flows, whenever rigid walls are set in a purely tangential motion. As shown, discontinuities on the tangential component of velocity are perfectly admissible and have no relationship with the compatibility condition to be satisfied by the normal velocity in truly multi-dimensional incompressible flows.

On the other side, there are several instances of multidimensional flows produced by an impulsive motion of the wall(s) such that the initial and boundary data do violate the compatibility condition for the normal component of velocity on the boundary. In these cases the original statement of the initial boundary value problem for incompressible flows is ill-posed and it is necessary to modify the initial velocity field conveniently to have compatible data, in the manner to be described below. As a result of this modification, a discontinuity between the tangential components of velocity of the modified initial condition and of the prescribed boundary values can be produced, but this occurrence does not jeopardize the well-posedness of the modified problem.

In conclusion, the same banner of 'impulsively started flows' is used to encompass two different classes of unsteady incompressible flows. The first class includes flows, with the first Stokes problem as the prototype, which are characterized by a discontinuity of the tangential velocity on the boundary at the initial time, and therefore are *ab initio* well-posed problems

not requiring any pre-processing of the initial and boundary data. The second class includes instead flows in which the impulsive motion of the boundary, or of some part of it, implies a violation of the compatibility condition for the normal component of velocity and therefore the ill-posedness of the corresponding mathematical problem. It is to this second class of flows that the airfoil problem here considered belongs to, since we have $\mathbf{n}\cdot\mathbf{v}_0|_{S_a} \neq \mathbf{n}\cdot\mathbf{b}_a|_{t=0}$, where $\mathbf{v}_0$ denotes the *incompatible* initial velocity.

3.3. Construction of compatible data

Let us suppose that the initial velocity field of the Navier–Stokes problem, denoted here $\mathbf{v}_0$, does not respect the compatibility conditions to be satisfied in incompressible flows, according to the previous analysis. For the sake of generality, we allow $\mathbf{v}_0$ to violate either the condition of solenoidality, i.e.

$$\boldsymbol{\nabla}\cdot\mathbf{v}_0 \neq 0$$

or the condition of compatibility between the initial and boundary data, i.e.

$$\mathbf{n}\cdot\mathbf{v}_0|_S \neq \mathbf{n}\cdot\mathbf{b}|_{t=0}$$

or both. Considering, for instance, an initial velocity field uniform in the whole fluid domain including the surface of the airfoils, we are violating the compatibility condition above since the velocity boundary value on the airfoil is necessarily zero at all times.

The consequence of using this combination of incompatible initial and boundary data in the numerical solution of the Navier–Stokes equations is illustrated in Figure 2 which shows a zoom of the velocity field computed at the second time step for $Re = 1000$ by the projection method to be described in Section 4.1. The non-sensical character of the computed flow field in the zoomed area including the vane and part of the main flap, is made evident by the occurrence of a velocity directed outward and inward the two sides of the main flap. We notice furthermore the presence of a strange stagnation point in the interior of the fluid, detached from the surface of the airfoil. Other unsatisfactory flow features, although less pronounced, are encountered near and around the other components of the multi-profile.

To have a well-posed problem, the initial (incompatible) velocity field $\mathbf{v}_0$ must be replaced by another vector field respecting the compatibility conditions. This can be achieved by simply resorting to the celebrated orthogonality theorem due to Ladyzhenskaya [6, Section 2, Theorem 1, p. 27]. The theorem states that every vector field of $\mathbf{L}^2(V)$ defined on any bounded simply connected domain $V \subset \mathbb{R}^2$ (or $\subset \mathbb{R}^3$) admits a unique orthogonal decomposition into a gradient field and a solenoidal field tangential to the boundary. The orthogonality is to be intended in the sense of the scalar product in the Hilbert space of square summable vector fields. In practical applications, for general non-zero normal velocity on the boundary the theorem is still effective although the decomposition is no more orthogonal.

Thus, we decompose any $\mathbf{v}_0 \in \mathbf{L}^2(V)$ as follows $\mathbf{v}_0 = -\boldsymbol{\nabla}\Psi + \mathbf{u}_0$, where $\mathbf{u}_0$ is a solenoidal vector field with a specified normal component on the boundary. The corrected initial velocity $\mathbf{u}_0$ is therefore given by $\mathbf{u}_0 = \mathbf{v}_0 + \boldsymbol{\nabla}\Psi$, where the scalar function Ψ is to be determined so that the two aforementioned conditions for $\mathbf{u}_0$ are satisfied. By substituting $\mathbf{u}_0$ in the compatibility conditions $\boldsymbol{\nabla}\cdot\mathbf{u}_0 = 0$ and $\mathbf{n}\cdot\mathbf{u}_0|_S = \mathbf{n}\cdot\mathbf{b}|_{t=0}$, we obtain

$$-\nabla^2\Psi = \boldsymbol{\nabla}\cdot\mathbf{v}_0, \quad \mathbf{n}\cdot\boldsymbol{\nabla}\Psi|_S = \mathbf{n}\cdot\mathbf{b}|_{t=0} - \mathbf{n}\cdot\mathbf{v}_0|_S \tag{15}$$

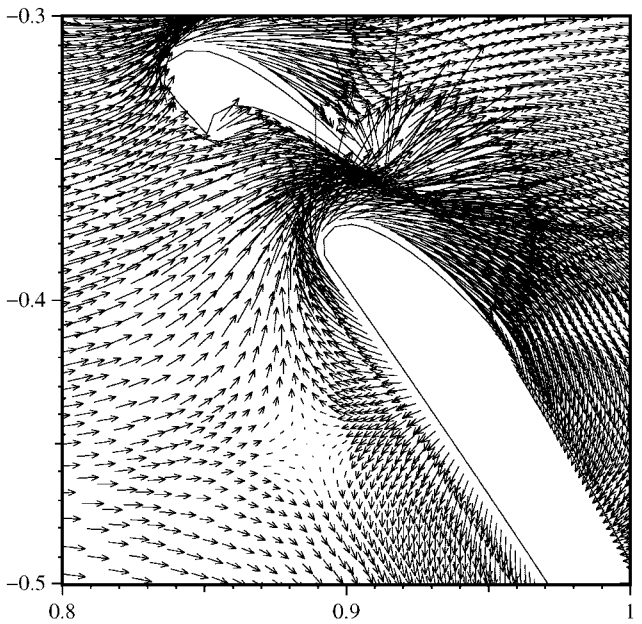

Figure 2. Particular of the velocity field after an impulsive start with incompatible data, at the second time step ($\Delta t = 0.001$) for $Re = 1000$.

This represents a Poisson equation for variable Ψ, supplemented by a Neumann boundary condition, whose solution yields the field $\boldsymbol{\nabla}\Psi$ for correcting the original initial velocity $\mathbf{v}_0$.

As far as the solvability of the Neumann problem for the Laplace operator is concerned, the source term and the boundary values of the normal derivative are subjected to a single, global, condition, which in the present situation reads

$$\int \boldsymbol{\nabla} \cdot \mathbf{v}_0 \, \mathrm{d}V = - \oint \mathbf{n} \cdot (\mathbf{b}|_{t=0} - \mathbf{v}_0|_S) \, \mathrm{d}S$$

This condition is satisfied thanks to the divergence theorem and since the boundary datum $\mathbf{b}$ respects the global constraint $\oint \mathbf{n} \cdot \mathbf{b} \, \mathrm{d}S = 0$ at $t = 0$, by the hypothesis. Thus, provided that the global condition of zero flux across the entire boundary is satisfied and once the original initial velocity $\mathbf{v}_0$ field has been replaced by $\mathbf{u}_0$, the data of the modified problem respect all of the compatibility conditions.

We observe that, when the initial velocity field $\mathbf{v}_0$ is already solenoidal but is not compatible with the boundary datum at time $t = 0$, the function Ψ represents actually the *potential* of a velocity correction to be added to $\mathbf{v}_0$: in this case Ψ can be denoted by Φ solution to the Laplace equation $\nabla^2 \Phi = 0$. If $\mathbf{v}_0$ is uniform, as in our airfoil problem where $\mathbf{v}_0 = \mathbf{U}$ in the whole domain, the compatible initial velocity field is given by $\mathbf{u}_0 = \mathbf{U} + \boldsymbol{\nabla}\Phi$. In this case, $\mathbf{u}_0$ turns out to be nothing but the potential velocity field past the profile associated with the uniform field $\mathbf{U}$ at large distance and a zero normal velocity on the profile (irrotational flow without circulation). In fact, for an impulsively started profile the initial velocity $\mathbf{v}_0$ is incompatible with the velocity boundary conditions, and we have: $\mathbf{v}_0 = \mathbf{U}$ in V, $\mathbf{u}|_{S_{\text{ext}}} = \mathbf{U}$ but

$\mathbf{u}|_{S_a} = 0$. As a consequence, the Neumann problem (15) becomes

$$\nabla^2 \Phi = 0, \quad \mathbf{n} \cdot \nabla \Phi|_{S_{ext}} = 0, \quad \mathbf{n} \cdot \nabla \Phi|_{S_a} = -\mathbf{n} \cdot \mathbf{U} \tag{16}$$

and therefore we have, on the one hand, $\mathbf{n} \cdot \mathbf{u}_0|_{S_{ext}} = \mathbf{n} \cdot (\mathbf{U} + \nabla \Phi)|_{S_{ext}} = \mathbf{n} \cdot \mathbf{U}$, and, on the other, $\mathbf{n} \cdot \mathbf{u}_0|_{S_a} = \mathbf{n} \cdot (\mathbf{U} + \nabla \Phi)|_{S_a} = 0$. In physical terms, the construction can be interpreted by saying that in an impulsively started flow the proper initial condition for the Navier–Stokes problem is determined by the potential flow that establishes itself instantaneously, by virtue of the incompressibility, in response to the sudden motion of the boundary. This interpretation corresponds precisely to the analysis by Lighthill [1, p. 80] and by Telionis [3, p. 81]. In Figure 3 (left) we represent the streamlines of the compatible initial velocity field $\mathbf{u}_0$.

Observing the flow field shown in Figure 3, we notice that the downstream stagnation points on all the airfoils, but for the slat, are not located at the trailing edges. This is a consequence of the fact that the initial velocity field has been assumed to be a potential flow. In other words, an arbitrariness in the choice of a compatible initial velocity exists whenever the flow domain is, as in the present case, multiply connected. In fact, there is an infinite number of inviscid incompressible flow fields in two dimensions satisfying the compatibility conditions which are characterized by the different values of the circulation around each airfoil. For instance, choosing these values so that the downstream stagnation points coincide with the trailing edges would lead to another compatible and mathematically admissible initial datum, which would be also in accordance with Kutta condition.

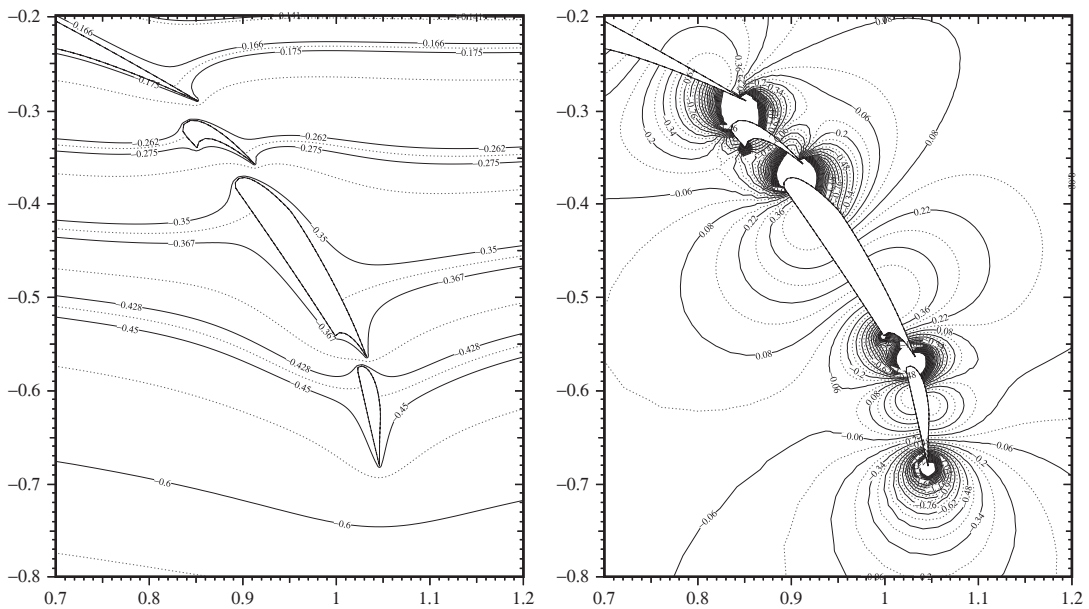

Figure 3. Streamlines (left) and Bernoulli pressure (right) of the initial flow after the construction of compatible data.

It should be noted that the modification of the initial velocity field, as anticipated in the previous section, can cause a discontinuity in the tangential components of the velocity on the boundary, namely, $\mathbf{n}\times\mathbf{u}_0|_S \neq \mathbf{n}\times\mathbf{b}|_{t=0}$. For an impulsive start, the discontinuity of the tangential component of the (compatible) initial velocity $\mathbf{u}_0$ on the boundary implies that a infinitely thin layer of infinite vorticity is present around the body at the initial time. This is the well-known phenomenon of vorticity generation on rigid boundaries. Such a discontinuity is allowed in the solution of the viscous incompressible problems, although it produces a blow up of the H^1 norm of the velocity solution as $t\to 0$, for details see Reference [16].

Finally, we present the pressure distribution associated with the compatible velocity field obtained by means of the proposed pre-processing of the initial velocity datum.

As a matter of fact, an initial condition for pressure is not required by the mathematical statement of incompressible flows. However, the numerical solution by means of an *incremental* fractional-step algorithm needs a starting pressure whenever the incremental scheme is used also at the *first* time step. According to our procedure for respecting the compatibility conditions, the modified velocity field at $t=0$ is determined by solving the Laplace equation. Therefore, we assume arbitrarily that Bernoulli's relation, valid for steady irrotational flows of an incompressible inviscid fluid, can be employed to characterize the starting pressure field, namely, $p_0+|\mathbf{u}_0|^2/2=C$, where C is an arbitrary constant (for a discussion about the choice of the initial pressure see Gresho [12, p. 736]). The application of this relation yields explicitly:

$$p_0(\mathbf{r})=-\frac{|\mathbf{u}_0(\mathbf{r})|^2}{2}+C=-\frac{|\mathbf{U}+\boldsymbol{\nabla}\Phi(\mathbf{r})|^2}{2}+C \tag{17}$$

The pressure field p_0 of the impulsively started flow past the penta-profile is shown in Figure 3 (right).

For the sake of completeness, recalling the Neumann boundary value problem (16) for the velocity potential Φ, its variational form is

$$\int_V \boldsymbol{\nabla} w\cdot\boldsymbol{\nabla}\Phi=\int_{S_{\text{ext}}} w\,\frac{\partial\Phi}{\partial n}+\int_{S_{\text{a}}} w\,\frac{\partial\Phi}{\partial n} \tag{18}$$

where the integration surface has been split in two parts S_{ext} and S_{a}. Substituting the boundary conditions on the right-hand side, the spatially discretized counterpart of the weak formulation of the problem (18) reads

Find $\Phi_h\in X_h\subset H^1(V)$ such that, for any test function $w_h\in X_h\subset H^1(V)$

$$(\boldsymbol{\nabla} w_h,\boldsymbol{\nabla}\Phi_h)=-\int_{S_{\text{a}}} w_h\,\mathbf{n}\cdot\mathbf{U} \tag{19}$$

For convenience, we are assuming that Φ_h is approximated by the same quadratic finite element interpolation that will be used for the velocity components in the projection method, as explained in the following section. From the so-computed solution Φ_h, we determine the compatible initial velocity field $\mathbf{u}_{h,0}$ on the triangulation through the relation $\mathbf{u}_{h,0}=\mathbf{U}+\boldsymbol{\nabla}\Phi_h$, which, once expressed in weak form, becomes: $(\mathbf{w}_h,\mathbf{u}_{h,0})=(\mathbf{w}_h,\mathbf{U}+\boldsymbol{\nabla}\Phi_h)$, for any vector function $\mathbf{w}_h\in\mathbf{X}_h\subset\mathbf{H}^1(V)$. This vector equation leads to two mass problems to determine the compatible initial velocity. From the nodal values of $\mathbf{u}_{h,0}$, the Bernoulli relation allows one to calculate the nodal values of the pressure of the initial potential flow: $p_{h,0}(\mathbf{r})=-|\mathbf{u}_{h,0}(\mathbf{r})|^2/2+C$. In

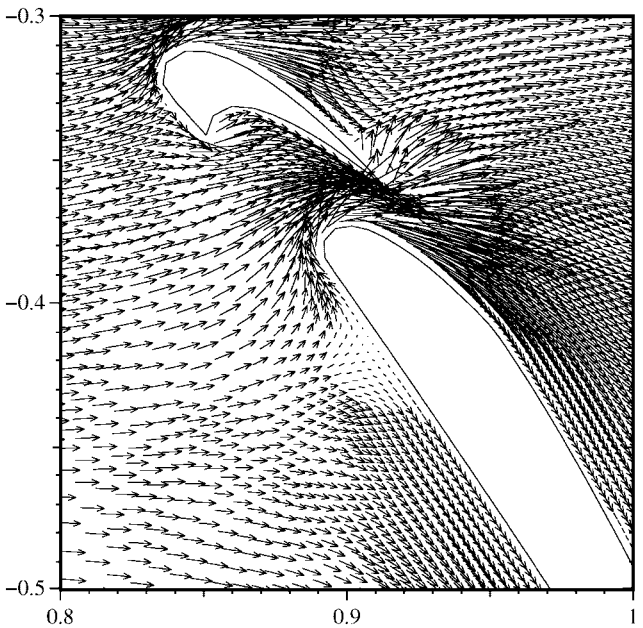

Figure 4. Particular of the velocity field after an impulsive start with compatible data, at the second time step ($\Delta t = 0.001$) for $Re = 1000$.

accordance with the analysis of the following section, this pressure field is linearly interpolated over the triangulation of the domain, to provide the initial pressure required at the first time step by the second-order incremental projection method, see below.

In Figure 4 we report the zoom of the velocity field for $Re = 1000$ computed by the projection method, starting from compatible initial and boundary data and using Bernoulli pressure as initial condition, at $t = 2\Delta t$, for $\Delta t = 0.001$. The behaviour of the flow field is in accordance with the physical expectations: a stagnation point is clearly seen on the upstream surface of the flap and the velocity near the two shown airfoils is found to posses the correct direction and intensity. The acceleration and flow development in the gap between the vane and flap is consistent with the effect of viscosity at the sharp trailing edge, which was not the case for the incompatibly started flow shown in Figure 2 at the same time step.

4. NUMERICAL METHOD

4.1. Second-order projection method

In this section we will briefly recall the incremental projection method of Guermond and Quartapelle [8, 9] used here to compute the impulsively started flows past airfoils. A detailed description of this projection method under general boundary conditions with convergence results and error estimates valid for spatial discretization by finite elements is given in References [8, 9]. An exhaustive analysis of the numerical properties of this scheme in the

context of the incremental projection method has been accomplished by Guermond in Reference [17]. In the same reference, the three-level BDF scheme has been selected as a very convenient time-marching method to benefit from better stability properties than those of the commonly used Crank–Nicolson scheme, which is only marginally stable. To guarantee an unconditional stability, i.e. to avoid any restriction on the time step Δt, the advection term $(\mathbf{u}\cdot\nabla)\mathbf{u}$ is replaced by its well-known skew-symmetric form $(\mathbf{u}\cdot\nabla)\mathbf{u}+\frac{1}{2}(\nabla\cdot\mathbf{u})\mathbf{u}$, evaluated semi-implicitly. In this way, the weak form of the momentum equation is guaranteed not to introduce any error in the kinetic energy of the spatially discrete solution. The unconditional stability of the second-order BDF scheme is maintained in the non-linear regime by approximating the new advection velocity $\mathbf{u}^{k+1}$ with its linearly extrapolated counterpart: $\mathbf{u}_\star^{k+1}=2\mathbf{u}^k-\mathbf{u}^{k-1}$, where the superscript index k refers to the time level t_k. The skew-symmetric form used in the numerical scheme will be:

$$(\mathbf{u}_\star^{k+1}\cdot\nabla)\mathbf{u}^{k+1}+\tfrac{1}{2}(\nabla\cdot\mathbf{u}_\star^{k+1})\,\mathbf{u}^{k+1}$$

The three-level BDF scheme will be used after the first two-level step in incremental form, leading, for $k\geqslant 1$, to the following advection–diffusion step:

$$\begin{gathered}\frac{3\mathbf{u}^{k+1}-4i^{\mathrm{t}}\hat{\mathbf{u}}^k+i^{\mathrm{t}}\hat{\mathbf{u}}^{k-1}}{2\Delta t}-\nu\nabla^2\mathbf{u}^{k+1}+(\mathbf{u}_\star^{k+1}\cdot\nabla)\mathbf{u}^{k+1}+\tfrac{1}{2}(\nabla\cdot\mathbf{u}_\star^{k+1})\mathbf{u}^{k+1}=-\nabla p^k\\ \mathbf{u}^{k+1}|_S=\mathbf{b}^{k+1}\end{gathered}\tag{20}$$

and to the incremental projection step of second-order time accuracy:

$$\begin{gathered}\frac{3\hat{\mathbf{u}}^{k+1}-3i\mathbf{u}^{k+1}}{2\Delta t}+\hat{\nabla}(p^{k+1}-p^k)=0\\ \hat{\nabla}\cdot\hat{\mathbf{u}}^{k+1}=0\\ \mathbf{n}\cdot\hat{\mathbf{u}}^{k+1}|_S=\mathbf{n}\cdot\mathbf{b}^{k+1}\end{gathered}\tag{21}$$

The final velocities $\hat{\mathbf{u}}^k$ and $\hat{\mathbf{u}}^{k-1}$ are eliminated from the solution algorithm. The advection–diffusion step for $k\geqslant 1$ takes the following form in practice:

$$\begin{gathered}\frac{3\mathbf{u}^{k+1}-4\mathbf{u}^k+\mathbf{u}^{k-1}}{2\Delta t}-\nu\nabla^2\mathbf{u}^{k+1}+(\mathbf{u}_\star^{k+1}\cdot\nabla)\mathbf{u}^{k+1}+\tfrac{1}{2}(\nabla\cdot\mathbf{u}_\star^{k+1})\mathbf{u}^{k+1}\\ =-\begin{cases}\nabla(3p^1-2p_0) & \text{for } k=1\\ \frac{1}{6}\nabla(14p^2-11p^1+3p_0) & \text{for } k=2\\ \frac{1}{3}\nabla(7p^k-5p^{k-1}+p^{k-2}) & \text{for } k\geqslant 3\end{cases}\\ \mathbf{u}^{k+1}|_S=\mathbf{b}^{k+1}\end{gathered}\tag{22}$$

and the projection step, formulated as a Poisson problem, reads:

$$\begin{gathered}-\hat{\nabla}^2(p^{k+1}-p^k)=-\frac{3}{2\Delta t}\nabla\cdot\mathbf{u}^{k+1}\\ \left.\frac{\partial(p^{k+1}-p^k)}{\partial n}\right|_S=0\end{gathered}\tag{23}$$

The two special expressions for the pressure extrapolation for $k=1$ and 2 in the advection–diffusion step are due to the elimination of the first end-of-step velocity by means of the special relation $\hat{\mathbf{u}}^1 = i,\ \mathbf{u}^1 + \Delta t\,\hat{\boldsymbol{\nabla}}(p^1 - p_0)$ of the first incremental projection step.

To develop the final solution algorithm, the two problems (22) and (23) are first recast in a variational form by means of the Galerkin method, by taking their scalar product with suitable weighting functions.‡ The weak equations are then written in a spatially discrete form by introducing a triangulation of the computational domain and approximated versions of the spaces for the (intermediate) velocity and the pressure.

The fully discrete weak form of the advection–diffusion step (22) reads:

For $k \geqslant 3$, find $\mathbf{u}_h^{k+1} \in \mathbf{X}_h$, with $\mathbf{u}_h^{k+1}|_S = \mathbf{b}^{k+1}$ such that, for all $\mathbf{v}_h \in \mathbf{X}_h$, with $\mathbf{v}_h|_S = 0$,

$$\begin{aligned}&\left(\mathbf{v}_h, \frac{3\mathbf{u}_h^{k+1} - 4\mathbf{u}_h^k + \mathbf{u}_h^{k-1}}{2\Delta t}\right) + \nu(\boldsymbol{\nabla}\mathbf{v}_h, \boldsymbol{\nabla}\mathbf{u}_h^{k+1})\\ &\quad + (\mathbf{v}_h, (\mathbf{u}_{h,\star}^{k+1}\cdot\boldsymbol{\nabla})\mathbf{u}_h^{k+1} + \tfrac{1}{2}(\boldsymbol{\nabla}\cdot\mathbf{u}_{h,\star}^{k+1})\mathbf{u}_h^{k+1})\\ &\quad = -\tfrac{1}{3}(\mathbf{v}_h, \boldsymbol{\nabla}(7p_h^k - 5p_h^{k-1} + p_h^{k-2}))\end{aligned} \tag{24}$$

Finally, the fully discrete form of the projection step (23) is

For $k \geqslant 1$, find $(p_h^{k+1} - p_h^k) \in N_h$ such that, for all $q_h \in N_h$,

$$(\boldsymbol{\nabla}q_h, \boldsymbol{\nabla}(p_h^{k+1} - p_h^k)) = -\frac{2}{3\Delta t}(q_h, \boldsymbol{\nabla}\cdot\mathbf{u}_h^{k+1}) \tag{25}$$

We assume a parabolic approximation for velocity and a linear approximation for pressure.

The second-order BDF projection scheme described above is completed by specifying the set of boundary conditions for velocity and pressure which are appropriate for the penta-profile problem considered here. To this purpose we truncate the infinite domain by a rectangle large enough to contain the multiple airfoil positioned nearly at the center of the region. The inflow, outflow, bottom and top sides of this rectangle will be denoted by S_{in}, S_{out}, S_{bottom} and S_{top}.

First of all, the no-slip condition on the airfoil is applied, i.e. $\mathbf{u}_h^{k+1}|_{S_a} = 0$. Then, from the hypothesis of a uniform $\hat{\mathbf{x}}$-oriented velocity field on the inflow side, we derive $\mathbf{u}_h^{k+1}|_{S_{\text{in}}} = \mathbf{U} = U\hat{\mathbf{x}}$. Furthermore, if the external boundary is supposed to be far enough from the airfoils, one can assume that no velocity perturbation in the $\hat{\mathbf{y}}$ direction exists on the frontiers, namely, $\boldsymbol{\tau}\cdot\mathbf{u}_h^{k+1}|_{S_{\text{out}}} = 0$, $\mathbf{n}\cdot\mathbf{u}_h^{k+1}|_{S_{\text{top}}\cup S_{\text{bottom}}} = 0$ and $\partial(\boldsymbol{\tau}\cdot\mathbf{u}_h^{k+1})/\partial n|_{S_{\text{top}}\cup S_{\text{bottom}}} = 0$. It is finally possible to resort to the incompressibility constraint and specify $\boldsymbol{\nabla}\cdot\mathbf{u}_h^{k+1}|_{S_{\text{out}}} = 0$ on the outflow boundary; this last condition, by virtue of $\boldsymbol{\tau}\cdot\mathbf{u}_h^{k+1}|_{S_{\text{out}}} = 0$, simplifies to the Neumann condition $\partial(\mathbf{n}\cdot\mathbf{u}_h^{k+1})/\partial n|_{S_{\text{out}}} = 0$, which is an uncoupled condition for the horizontal velocity.

‡We use the scalar product notation for scalar functions $(q,p) \equiv \int_V qp\,\mathrm{d}V$ as well as for vector functions $(\mathbf{v},\mathbf{u}) \equiv \int_V \mathbf{v}\cdot\mathbf{u}\,\mathrm{d}V$. Moreover, we define also $(\boldsymbol{\nabla}\mathbf{v}, \boldsymbol{\nabla}\mathbf{u}) \equiv \int_V \sum_{i=1}^d \sum_{j=1}^d (\partial v_j/\partial x_i)(\partial u_j/\partial x_i)\,\mathrm{d}V$, where $d=2$ (or $d=3$) is the number of spatial dimensions.

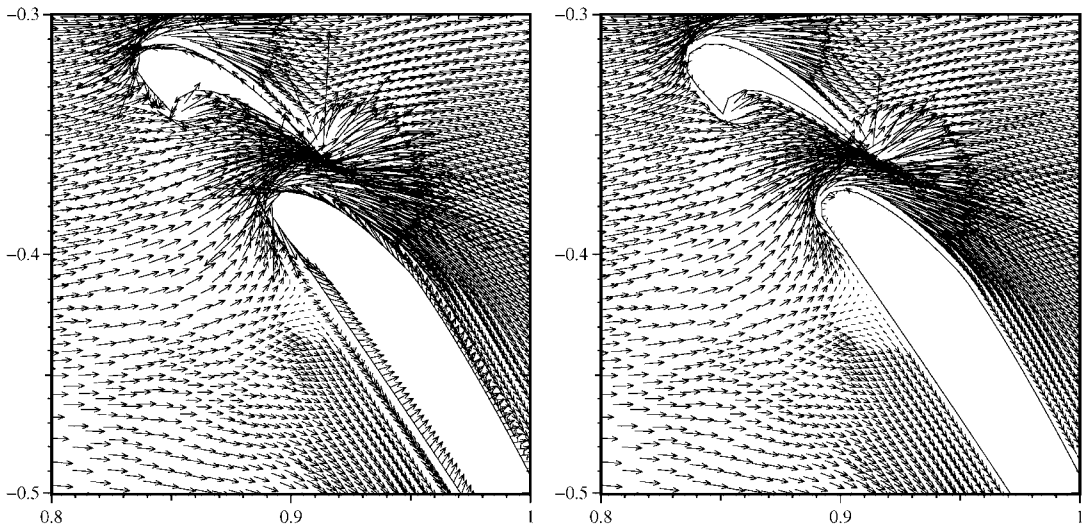

Figure 5. Particular of the velocity field after an impulsive start for $Re = 1000$. Representation of the end-of-step velocity $\hat{\mathbf{u}}_h^2$ at the second time step ($\Delta t = 0.001$). Left plot: incompatible data; right plot: compatible data.

The Poisson equation of the projection step is supplemented by a Dirichlet condition for the pressure on the outflow side, $p^{k+1} = 0$, and a homogeneous Neumann condition on the remaining part of the boundary, namely, on $S_{\text{in}} \cup S_{\text{top}} \cup S_{\text{bottom}} \cup S_{\text{a}}$.

Incidentally, it is interesting to verify how the ill-posedness affects also the end-of-step velocity generated by the projection method. The examination of the shots taken at $t = 2\Delta t = 0.002$ shows that the end-of-step solution computed starting from incompatible data (left plot of Figure 5) has an even worse behaviour than the intermediate velocity computed under the same initial conditions (Figure 2 of Section 3.3). First, the boundary condition on velocity is violated by both the normal and tangential components. This is a consequence of having contrived artificially the end-of-step velocity within a space of too high a regularity. In fact, for instance, the field $\hat{\mathbf{u}}_h^2$ given by relation

$$\hat{\mathbf{u}}_h^2 = i,\ \mathbf{u}_h^2 - \frac{2\Delta t}{3}\hat{\boldsymbol{\nabla}}(p_h^2 - p_h^1)$$

is evaluated in the same space of $\mathbf{u}_h^2$ by means of the weak equivalent of this equation. This amounts to solve two mass matrix problems for the Cartesian components of the velocity on the parabolic grid.

Moreover, a fully unphysical backward velocity of the fluid is observed near the front edge of the main flap. The intermediate and end-of-step velocity fields obtained starting from compatible data can be compared by examining the right plot of Figure 5 with the plot of Figure 4. In the leading-edge regions we notice that the end-of-step velocity field shows a slight mismatch with the correct zero boundary condition.

The comparison clearly illustrates the fundamental role of the step used to enforce compatibility, even for the end-of-step velocity which does not satisfies the zero velocity condition at the leading edge of the airfoils due to the aforementioned reasons.

This section is concluded by a brief explanation of the method used to evaluate the vorticity field and the streamlines, which are useful to represent the fluid motion caused by the impulsive start of the multi-profile. At any time the vorticity is simply given by the definition $\boldsymbol{\omega} = \boldsymbol{\nabla} \times \mathbf{u}$, which in two dimensions can be written in discretized weak form as: $(w_h, \omega_h) = (w_h, \hat{\mathbf{z}} \cdot \boldsymbol{\nabla} \times \mathbf{u}_h)$. Given the velocity field $\mathbf{u}_h^{k+1}$, the finite element equations are expressed by the linear system $M\boldsymbol{\Omega}^{k+1} = \mathbf{F}^{k+1}$, where M is the mass matrix, $\boldsymbol{\Omega}^{k+1}$ is the unknown vector of the nodal values of vorticity and $\mathbf{F}^{k+1}$ is the L^2 projection of $\hat{\mathbf{z}} \cdot \boldsymbol{\nabla} \times \mathbf{u}_h^{k+1}$ onto the space of the test functions.

On the other hand, any solenoidal velocity field $\mathbf{u}$ in two dimensions can be expressed in terms of a scalar function ψ, called *stream function*, according to $\mathbf{u} = \boldsymbol{\nabla}\psi \times \hat{\mathbf{z}}$, namely, in terms of the velocity components: $u = \partial\psi/\partial y$ and $v = -\partial\psi/\partial x$. Taking the curl of this relation leads to the Poisson equation for the stream function $-\nabla^2\psi = \hat{\mathbf{z}} \cdot \boldsymbol{\nabla} \times \mathbf{u}$. The discretized weak form of this equation is $(\boldsymbol{\nabla} w_h, \boldsymbol{\nabla}\psi_h^{k+1}) = (w_h, \hat{\mathbf{z}} \cdot \boldsymbol{\nabla} \times \mathbf{u}_h^{k+1}) + \int_S w_h \, (\partial\psi_h^{k+1}/\partial n) \, \mathrm{d}s$, where the surface integral depends on the kind of the boundary conditions, which are deduced from the value assumed by the velocity on the boundary S, namely, from $\mathbf{u}|_S = \mathbf{b}$. The velocity vector $\mathbf{b}$ being known on S, it provides two different boundary conditions for ψ_h^{k+1}: the normal component gives $\partial\psi_h^{k+1}/\partial s|_S = \mathbf{n} \cdot \mathbf{b}^{k+1}$, while the tangential component implies $\partial\psi_h^{k+1}/\partial n|_S = -\boldsymbol{\tau} \cdot \mathbf{b}^{k+1}$. Correspondingly, two alternative boundary value problems can be formulated for the scalar unknown ψ_h^{k+1}. The former is a Poisson equation supplemented by Dirichlet conditions on the boundary but for the outflow side S_{out}, while the latter is an equation supplemented by Neumann conditions on the entire boundary. As well-known, the constant value assumed by the stream function on each airfoil of the multi-profile is related to the mass rate of fluid passing between the airfoils and is given by a line integral of the velocity field. Only after these values have been computed, the boundary data of the Dirichlet problem are complete. We have solved both the Dirichlet and the Neumann boundary value problem. The stream values on the airfoils provided by the two alternative formulations yield to a difference less than 4 percent.

4.2. Post-processing procedure

The solution of the projection method is affected by a time-splitting error due to the fractional-step nature of the time discretization scheme. It is therefore worthwhile to investigate whether it is possible to compute a pressure field affected by a smaller error of this nature by resorting to an 'unsplit' form of the momentum equation.

Actually, once the velocity field has been computed, we can consider the momentum equation with the pressure gradient taken as unknown, rather than evaluating this term explicitly from the extrapolated pressure field of the projection step. By expressing the viscous term as the double curl of the velocity solution to the projection method, the momentum equation can be used to obtain a weak form of an elliptic problem for pressure which embodies homogeneous Neumann boundary condition, quite naturally. It is important not to confuse this (weak) elliptic problem with the (strong) Poisson equation for pressure which could be derived by taking the divergence of the momentum equation and exploiting the incompressibility condition. The solution of the Poisson equation would in fact require boundary conditions for

pressure. As well-known, such conditions do not exist for the continuum problem and are difficult to be achieved in the discrete case, particularly when a spatial approximation of local type is employed, as in the present work.

Following this reasoning, let us consider the momentum equation for two-dimensional flows with the viscous term written as the double curl of the velocity, namely,

$$\frac{\partial \mathbf{u}}{\partial t} + (\mathbf{u}\cdot\nabla)\mathbf{u} = -\nabla p - \nu\nabla\times\nabla\times\mathbf{u} \tag{26}$$

Multiplying this equation by ∇v, $\forall v \in H^1(V)$, integrating by parts the first term, using the incompressibility condition $\nabla\cdot\mathbf{u}=0$ and the velocity boundary condition for the normal component, we obtain

$$(\nabla p, \nabla v) = -((\mathbf{u}\cdot(\nabla)\mathbf{u}, \nabla v) + \nu \oint_S \nabla\times\mathbf{u}\ \boldsymbol{\tau}\cdot\nabla v\,\mathrm{d}S - \oint_S \frac{\partial(\mathbf{n}\cdot\mathbf{b})}{\partial t} v\,\mathrm{d}S \tag{27}$$

$\forall v \in H^1(V)$. This equation can be solved to determine the pressure field $p = p^k$ at time t_k from the velocity $\mathbf{u}=\mathbf{u}^k$ and vorticity $\omega=\omega^k$ (here $p=p^k$ should not be confused with that generated by the projection method). There is still an open question: what is the more appropriate approximation for the new pressure? Looking at Equation (27), all integrands in the right-hand side are given by a parabolic approximation but, as remarked before, the pressure in incompressible flows cannot be of the same regularity as velocity. The convergence tests which follow, based on the exact solution (28), suggest a possible answer to the question, although we will make no attempt here in the direction of a mathematical proof.

4.3. Convergence tests

The theoretical second order accuracy of the three-level BDF scheme [17] can now be checked by numerical tests on the following analytical solution in the unit square $\Omega=[0,1]^2$:

$$\begin{aligned} u_{\mathrm{ex}} &= -\cos x \sin y\, g(t) \\ v_{\mathrm{ex}} &= \sin x \cos y\, g(t) \\ p_{\mathrm{ex}} &= -\tfrac{1}{4}[\cos(2x)+\cos(2y)]g^2(t) \end{aligned} \tag{28}$$

where $g(t)=\sin(2t)$. Setting the velocity in the form $\mathbf{u}_{\mathrm{ex}}=\bar{\mathbf{u}}(x,y)\ g(t)$, the source term corresponding to the Navier–Stokes equation is $\mathbf{f}=\bar{\mathbf{u}}(x,y)[g'(t)+(2g(t)/Re)]$. The Reynolds number is set to 100 and two meshes composed, respectively, by 2×20^2 and 2×40^2 triangles are used. Figure 6 shows the maximum value in time, over $0\leqslant t\leqslant 1.5$, of the error in L^2 norms for the pressure and the error in H^1 and L^2 norms for the velocity. Comparing the curves with the second order slope plotted in the figures, we can appreciate the accordance between the theory and the numerical tests. The different saturations of the errors as $\Delta t\to 0$ are due to the spatial discretization error, which is of order h^2 for the velocity in the H^1 norm and h^3 in the L^2 norm, of order h^3 for the pressure in the L^2 norm.

In Figure 7 we plot the errors in the L^2 norm for three different pressure fields at $t=1$ obtained by means of the projection method (linear) and by means of the spatially discrete version of Equation (27) with a linear or parabolic approximation over the same grids employed for the previous convergence test. The order of accuracy in time of both new pressure

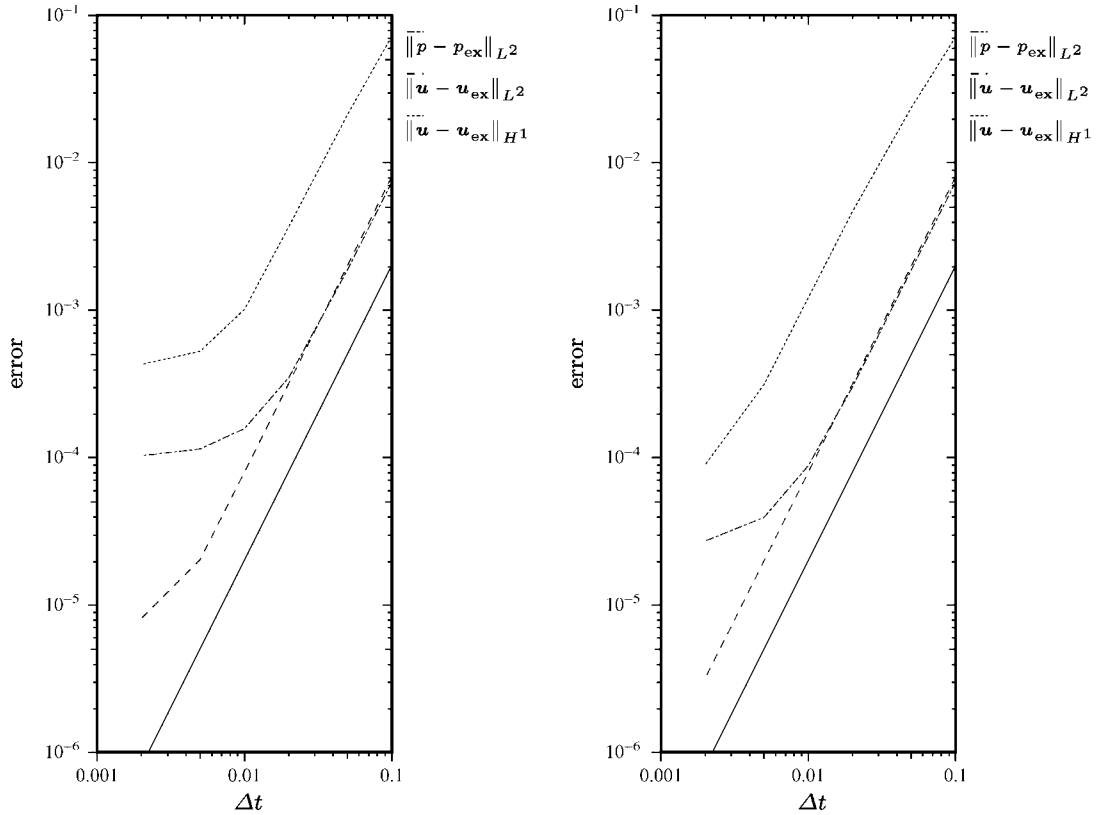

Figure 6. Convergence tests for the second order BDF projection method. Analytical test problem with $Re = 100$. Finite element meshes of 2×20^2 (left) and 2×40^2 (right) triangles.

fields is the same as in the projection method, with a smaller error constant in both cases. A more evident improvement emerges looking at the saturation of the error due to the spatial discretization: the linear approximation saturates to a value only slightly smaller than the one of the projection method, while the saturation value of the parabolic approximation is smaller by more than one order of magnitude. In the next section the new pressure fields over the penta-profile will be computed to assess the relevance of this convergence test for actual simulations.

5. SOME COMPARISONS

The aim of this section is to compare the numerical results of the projection method with those obtained by the weak ψ-ω (harmonic) formulation presented in Reference [10] and to analyse the influence of the procedure for the compatibility as the time of the solution goes on. The aerodynamic configuration considered in that work is the same that we have adopted in the present study. We perform calculations with the same value of $Re = 1000$ and

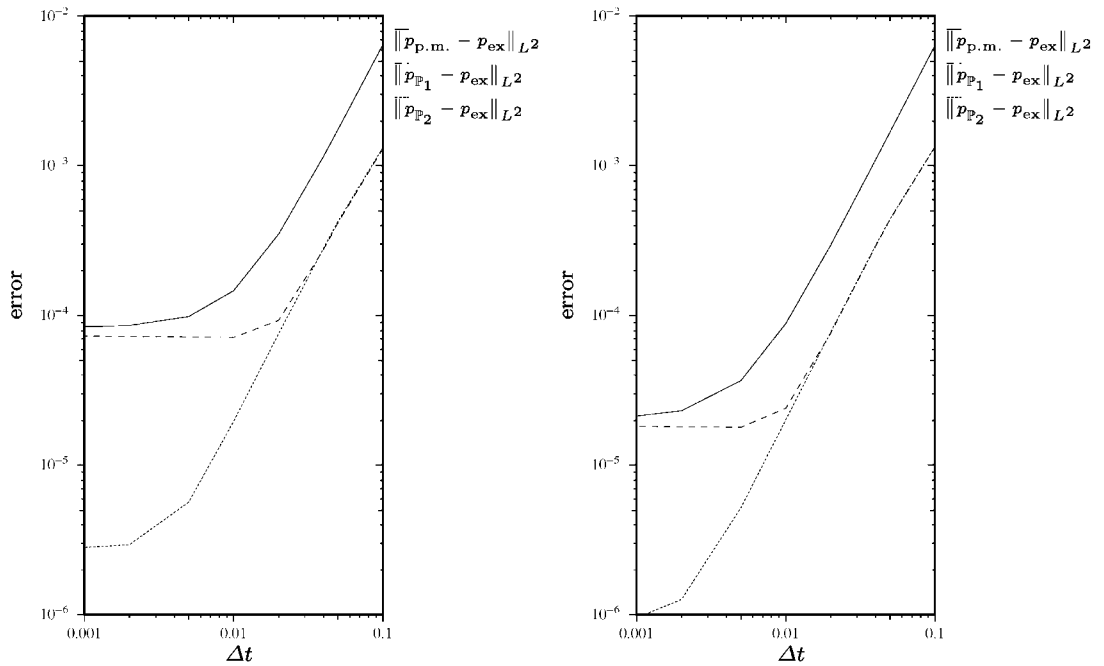

Figure 7. Convergence tests for the pressure. Analytical test problem with $Re = 100$. Finite element meshes of 2×20^2 (left) and 2×40^2 (right) triangles. The notation $p_{\mathrm{p.m.}}, p_{\mathbb{P}_1}, p_{\mathbb{P}_2}$ stands, respectively, for the pressure of the projection method and the pressure calculated by means of the 'unsplit' momentum equation (27) with linear and parabolic interpolations.

an equivalent mesh consisting of about 14 800 triangles to be compared with the mesh of 15 000 triangles employed in Reference [10].

In Figure 8, the streamlines and the vorticity field are presented: the variables ψ and ω are not unknowns of the projection method and have been calculated from the velocity field $\mathbf{u}_h^{k+1}$ as described at the end of Section 4.1. The agreement between the solutions obtained by the two completely different numerical schemes exceeds our best expectations.

Another interesting comparison can be done for the pressure coefficient $c_p \equiv (p - p_\infty)/\frac{1}{2}U^2$. As clearly shown in Figure 9 (top), a remarkable difference of the solutions is primarily concentrated on the lower surface of the airfoils where the coefficient of pressure deduced from the projection method exceeds the value 1 which is characteristic for a stagnation point. A possible justification of this discrepancy is that the pressure field is affected by the time-splitting error due to the particular 'half-stepping' scheme employed in the projection method.

In the middle and bottom plots of the same Figure 9 the c_p curves of the post-process pressure fields based on respectively linear and parabolic interpolations are compared with the reference results by the ψ-ω algorithm. The linear pressure has an agreement with the reference c_p very similar to that just seen for the (linear) pressure of the projection method, but now the value of c_p on the lower surface is slightly underestimated instead of overestimated. The size of these differences is however comparable, in conformity with the pres-

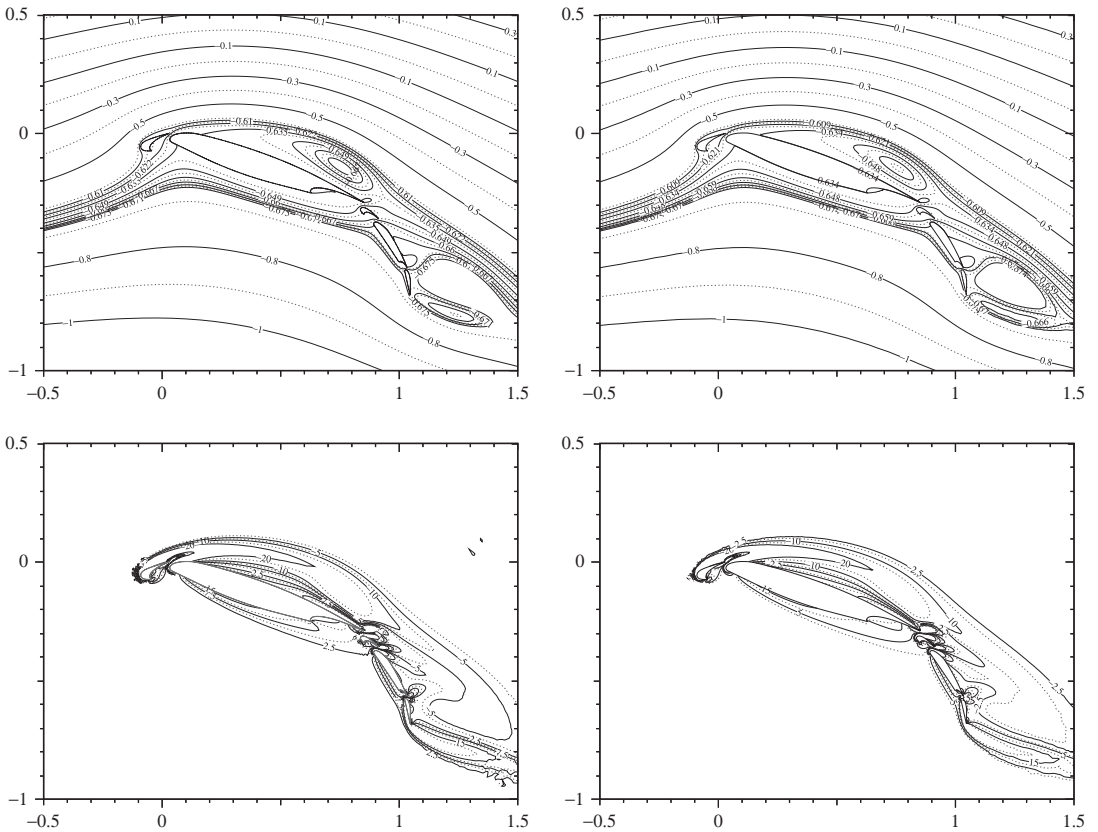

Figure 8. Streamlines (top) and vorticity (bottom) for $Re = 1000$ at $t = 2$. Left: solution obtained by the projection method. Right: solution obtained by the ψ-ω harmonic method [10].

sure errors found for the analytical test case of Section 4.3, see Figure 7. The comparison for the parabolic pressure is much more satisfactory, particularly on lower surface of the airfoils. The conclusion is that the more expensive parabolic interpolation for the pressure of the post-processing phase yields the highest accuracy among the three considered pressures, as predicted by the error analysis and the numerical tests conducted in the previous section.

Finally, it is worthwhile to analyse the different evolution of solutions provided by the projection method starting from compatible and incompatible initial data, in the course of the simulation. In Figure 10 we plot this difference in L^2 and H^1 norms for the velocity and in L^2 norm for the pressure. In the first iterations the difference is remarkable especially for the pressure and becomes obviously smaller as k increases. Therefore if one is not interested to the solution at the first iterations of the simulation the pre-processing procedure is not strictly necessary. Nevertheless incompatible initial data could cause the numerical method to diverge at the first iterations.

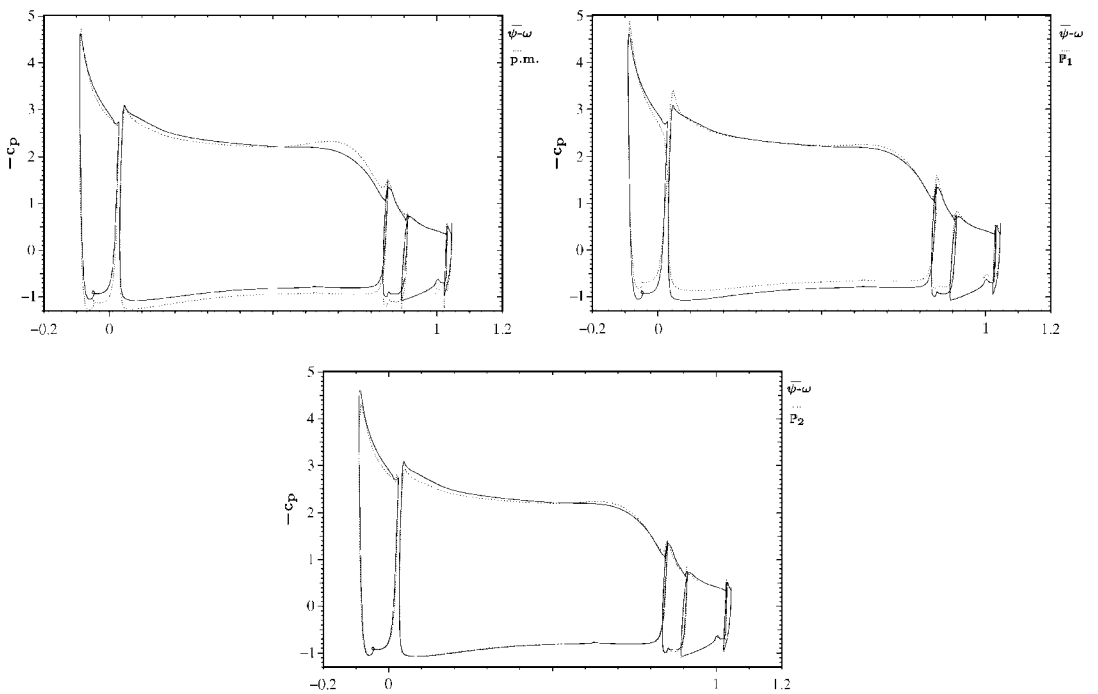

Figure 9. Pressure coefficient on the multi-profile airfoil for $Re = 1000$ at $t = 2$. Top: comparison of the solution by the projection method with the solution by the ψ-ω method [10]. Middle and bottom: pressure evaluated directly from the momentum equation projected onto ∇H^1 with $\mathbb{P}_1$ and $\mathbb{P}_2$ approximations respectively, compared to the ψ-ω solution [10].

6. CONCLUSIONS

This work has demonstrated that the integration of the time-dependent Navier–Stokes equations for the primitive variables by a numerical method requires a proper analysis of the issue of the compatibility of the initial and boundary data for the velocity. Although the mathematical principles underlying such compatibility conditions are fixed in the most established theoretical literature on the Navier–Stokes equations, their implications on the numerical side have often been underestimated. In the particular case of a velocity on the boundary increasing smoothly with the fluid at rest initially, disregarding the compatibility between the boundary and initial conditions has no consequences, as it is trivially satisfied, both data being null on the boundary at $t = 0$. On the contrary, when an immersed body is started instantaneously, the analysis of the compatibility is mandatory for developing a proper numerical scheme free from a pathological behaviour in the start-up phase of the fluid motion. To realize the precise meaning of an impulsively started flow, we have considered the first Stokes problem and have shown that it represents a degenerate kind of impulsive start inadequate to illustrate the ill-posedness of problems where walls of arbitrary shape are suddenly set in motion with a velocity component normal to their surface.

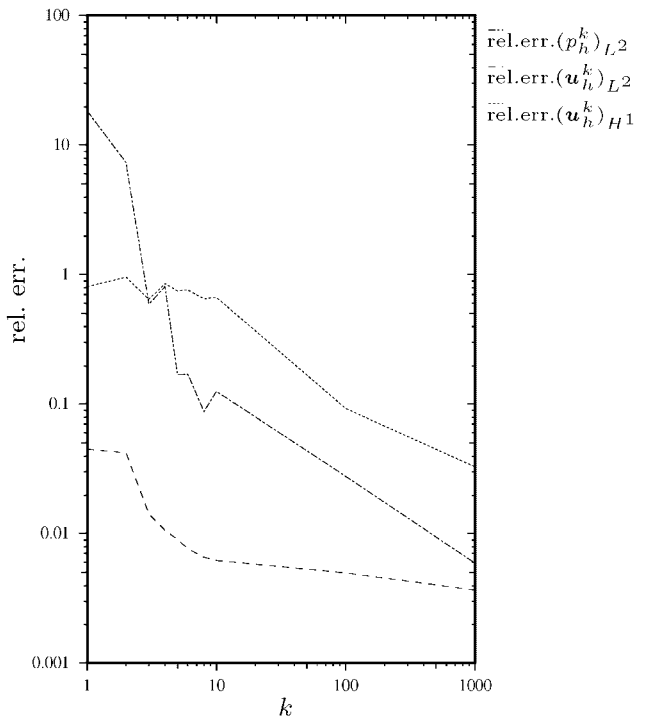

Figure 10. Error between the solutions with compatible ($\mathbf{u}_h^k$) and incompatible ($\tilde{\mathbf{u}}_h^k$) initial data over the iterations k. Solutions obtained with the projection method, $Re = 1000$ and $\Delta t = 0.001$. The notation for the relative error means rel.err. $(f_h^k)_{\text{norm}} = \|f_h^k - \tilde{f}_h^k\|_{\text{norm}} / \|f_h^k\|_{\text{norm}}$.

In this work we have introduced a procedure for enforcing the compatibility in flows within an arbitrarily shaped two-dimensional region, that modifies the initial velocity field to ensure the matching between the normal components of the initial velocity and of the boundary condition at $t = 0$, so as to guarantee the well-posedness of the initial-boundary value problem for incompressible flows. The cost of such a procedure is that of solving a simple Poisson equation for a velocity potential in a pre-processing phase of the calculations. This procedure restoring the compatibility has been developed to complement a projection method of incremental type which uses a second-order BDF time discretization and a finite element spatial discretization [8, 9]. The first time step of the incremental scheme involves the pressure field at $t = 0$, and it has been shown that the Bernoulli pressure associated with the stationary flow of the compatible initial velocity can be employed successfully to account for the pressure build-up in impulsively started flows. We have also introduced the idea of post-processing the velocity solution provided by the projection method. A pressure field alternative to that given by the projection step can in fact be obtained from the velocity solution of the projection method, considering linear or quadratic interpolations.

As a representative example, we have applied the projection method to the simulation of the flow past a multiple airfoil, to compare our solutions with those provided by other methods. The correctness of all the algorithms implemented here has been verified by comparing the

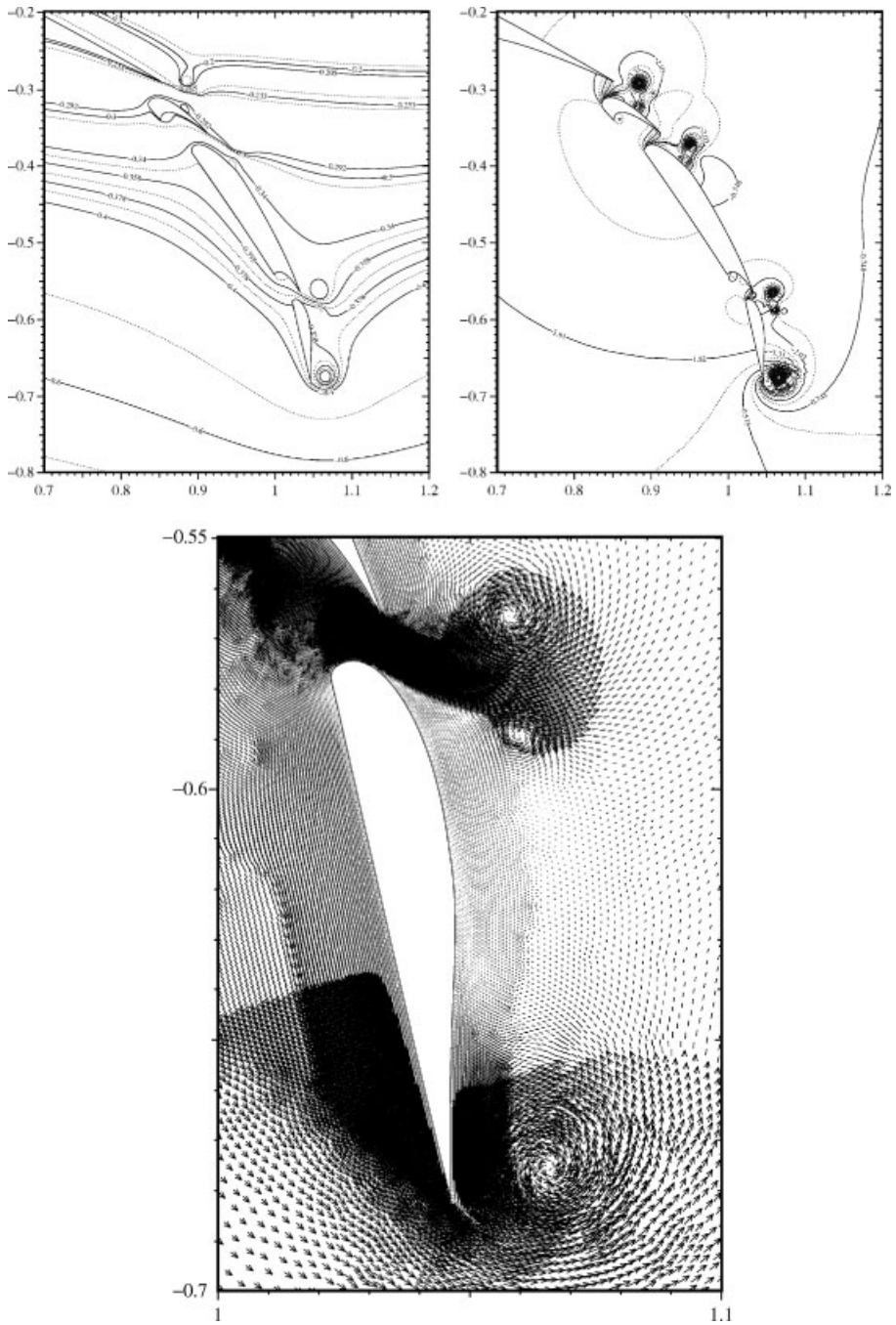

Figure 11. Starting vortices leave the trailing edges of the penta-profile at $t = 0.02$ for $Re = 10\,000$. Top: streamlines (left) and pressure field (right). Bottom: velocity field.

solution of the projection method for $Re = 1000$ with results provided by a completely different numerical method for solving the Navier–Stokes equations in two dimensions using non-primitive variables [10]. The comparison of the streamlines near the multi-profile on the airfoil surfaces, for a geometrical configuration characterized by sharp trailing edges and by the vertical incidence of the auxiliary flap, has been found to be fully satisfactory, especially considering the occurrence of several recirculating bubbles and the massive separation. As far as the pressure coefficient is concerned, we have shown that the alternative pressure field based on the parabolic approximation yields the best agreement with the pressure field extracted from the solution to the non-primitive variable equations.

The agreement has been carefully checked at times not very close to the beginning of the motion, since for very small t an accurate representation of the starting vortex(ices) would require a specific modelling in the region of the trailing edge(s), which was outside the scope of the present work. Nevertheless, in Figure 11 we report the starting vortices near four trailing edges of the multi-profile for $Re = 10\,000$ at an early time $t = 0.04$. The expected starting vortices have been already formed and are correctly drawn downstream. In any case, before trying to modify or enrich the mathematical model for handling complicated physical situations like those shown by the figure, we feel important and highly recommendable to check the coherence of the mathematical statement of the unsteady incompressible problem so that it can be continuously solvable in the sense of Hadamard. Only after this preliminary logical step has been overcome, one can hope to represent the original viscous incompressible fluid dynamic problem in a discrete form with an increasing order of accuracy both in space and in time.

REFERENCES

1. Lighthill J. *An Informal Introduction to Theoretical Fluid Mechanics*. Clarendon Press: Oxford, 1986.
2. Rosenhead L. *Laminar Boundary Layers*. Oxford University Press: Oxford, 1963.
3. Telionis DP. *Unsteady Viscous Flows*, Springer Series in Computational Physics. Springer-Verlag: New York, 1981.
4. Karamcheti K. *Principles of Ideal–Fluid Aerodynamics*. Wiley: New York, 1966.
5. Ashley H, Landahl M. *Aerodynamics of Wings and Bodies*. Dover Publications, Inc.: New York, 1965.
6. Ladyzhenskaya OA. *The Mathematical Theory of Viscous Incompressible Flow*. Gordon and Breach: New York, 1969.
7. Temam R. *Navier–Stokes Equations. Theory and Numerical Analysis*, Studies in Mathematics and its Applications, vol. 2. North-Holland: Amsterdam, 1977, AMS Cheslea Publishing: Providence, RI, 2000.
8. Guermond J-L, Quartapelle L. Calculation of incompressible viscous flows by an unconditionally stable projection FEM. *Journal of Computational Physics* 1997; **132**:12–33.
9. Guermond J-L, Quartapelle L. On the approximation of the unsteady Navier–Stokes equations by finite element projection methods. *Numerische Mathematik* 1998; **80**:207–238.
10. Biava M, Modugno D, Quartapelle L, Stoppelli M. Weak ψ-ω formulation for unsteady flows in 2D multiply connected domains. *Journal of Computational Physics* 2002; **177**:209–232.
11. Adams R. *Sobolev Spaces* (2nd revised edn). Academic Press: New York, 2003.
12. Gresho PM, Sani RL. *Incompressible Flow and Finite Element Method*. Wiley: Chichester, England, 1998.
13. Kato T. On classical solutions of the two-dimensional non-stationary Euler equations. *Archive for Rational Mechanics and Analysis* 1967; **25**:188–200.
14. Taylor ME. *Partial Differential Equations*, vol. III. Springer-Verlag: New York, 1999.
15. Lamb, Sir Horace. *Hydrodynamics* (6th edn). Dover Publications, Inc.: New York, 1932.
16. Guermond J-L, Quartapelle L. Equivalence of **u**-p and ζ-ψ formulations of the time-dependent Navier–Stokes equations. *International Journal for Numerical Methods in Fluids* 1994; **18**:471–487.
17. Guermond J-L. Un résultat de convergence à l'ordre deux en temps pour l'approximation des équations de Navier–Stokes par une technique de projection. *Modél. Math. Anal. Numér.* (M^2AN) 1999; **33**:169–189.

